Interface of a Bi(001) film on Si(111)-7 × 7 imaged by surface x-ray diffraction

Tetsuroh Shirasawa,* Masanori Ohyama, Wolfgang Voegeli, and Toshio Takahashi
Institute for Solid State Physics, University of Tokyo, 5-1-5 Kashiwanoha, Kashiwa 277-8581, Japan
(Received 7 June 2011; published 3 August 2011)

We show structural characteristics of an epitaxial Bi(001) film on the Si(111)-7 × 7 surface, including its atomic-layer-resolved interface, which were revealed by surface x-ray diffraction and direct methods of structure analysis. The lattice constants of a 6-nm-thick Bi(001) film at room temperature were determined to be $a = 4.50 \pm 0.02$ Å and $c = 11.96 \pm 0.04$ Å in the hexagonal coordination, which are compressed by 0.9% and are expanded by 0.8%, respectively, from the bulk structure. The coexistence of two rotational domains, related by a 180° rotation around the c axis to one another, was observed in all samples. The wetting layer of Bi, between the film and the substrate, was directly reconstructed by a holographic method, and the electron-density profile along the c axis was obtained by phase-retrieval methods. The spacing between the wetting layer and the film is wider than the spacing between the (001) bilayers by 36%. The film maintains its bulklike structure, except for small vertical relaxations of the top and bottom layers. These structural properties indicate that the film is nearly free standing without breaking the structural-inversion symmetry between the top and the bottom as expected from its electronic properties.

DOI: 10.1103/PhysRevB.84.075411 PACS number(s): 61.05.cp, 68.35.Ct

I. INTRODUCTION

Bi, in reduced dimensionality, has attracted research interest for the past several decades. Because of its large Fermi wavelength and long mean-free path,[1] downsized Bi has provided good opportunities for studying quantum size effects.[2,3] One of the recent hot topics is the spin splitting of energy bands at surfaces of Bi, caused by the lack of structural inversion symmetry across the vacuum-surface interface, the so-called Rashba effect.[4–9] The strong spin-orbit interaction owing to the heavy mass of Bi makes its surfaces attractive subjects for studying large spin-splitting bands on a surface of nonmagnetic material. Highly crystalline Bi films on the Si(111)-7 × 7 surface,[10] with the [001]-crystal orientation along the surface normal (see Fig. 1), are a good system to study the Rashba effect,[7,9,11] the quantum size effect,[12] and their interplay.[13] The surface states of Bi(001) films have the spin-splitting energy bands,[7] but quantum well states extending throughout the film do not show Rashba-type spin splitting.[12,13] The lack of Rashba splitting is attributed to the structural inversion symmetry between the vacuum-film and the film-substrate interfaces. Very recently, the spin-split surface bands were reported to show interesting symmetry-related characteristics, which deviate from the conventional picture of the Rashba effect.[9]

Upon deposition on the Si(111)-7 × 7 surface at room temperature, first, {012}-oriented Bi islands with random in-plane orientation are formed, and then, the film is transformed into a [001]-oriented single-crystal phase above a critical thickness of ∼2.5 nm. The Bi(001) film has a magic epitaxial relationship with the substrate; a 6 × 6 lattice of Bi(001) matches with the Si(111)-7 × 7 lattice.[10] Thanks to the easiness of preparation of high-quality crystalline film, the Bi(001) film also has been utilized as a host material to create a topological insulator[14] and as a template for the growth of crystalline pentacene organic films.[15]

Although its interesting electronic properties and the use as a host or template material are strongly related to its structural properties, a detailed structural analysis of the film, including its buried interface, has not been reported yet. Scanning tunneling microscopy (STM) studies showed the formation of a wetting layer at the initial stage of deposition,[16,17] however, its existence at the buried interface has not been confirmed. Even though a transmission electron microscopy (TEM) study directly imaged the interface,[18] details of the interface image have not been discussed.

This paper presents structural properties of the Bi(001) film and its interface with atomic-layer resolution, investigated with surface x-ray diffraction (XRD). The nominal lattice constants were obtained for a 6-nm-thick film. We observed the coexistence of rotational domains that were related by 180° rotation in all samples. The electron-density profile across the interface, revealed by recently developed direct methods in surface-interface crystallography, clearly shows the wetting layer in the buried interface. The obtained structure model explains the TEM image and the free-standing nature of the film well.

II. EXPERIMENTAL METHOD

Sample preparation and *in situ* XRD experiments were performed with the surface diffractometer equipped with an ultrahigh vacuum chamber at beamline 15B2 of the Photon Factory at High Energy Accelerator Research Organization (KEK). The base pressure of the chamber was 1×10^{-8} Pa. An n-type Si(111) wafer ($\rho \sim 0.02\ \Omega\,\mathrm{cm}$) was used as the substrate. The substrate surface was repeatedly cleaned by resistive heating at 1250 °C until a sharp 7 × 7-reflection high energy electron diffraction pattern was observed. Bi was deposited onto the 7 × 7 surface at room temperature. With the definition of a Bi(001) bilayer shown in Fig. 1, the deposition rate was ∼0.3 bilayer/min. During the deposition, the vacuum was about 1×10^{-7} Pa. After the deposition, we annealed the sample at ∼150 °C for 30 min to smooth its surface.[15]

XRD measurements were preformed at room temperature with an x-ray energy of 11 keV. Integrated intensities along reciprocal lattice rods were measured and were corrected for scattering geometry, polarization, and active sample area.[20]

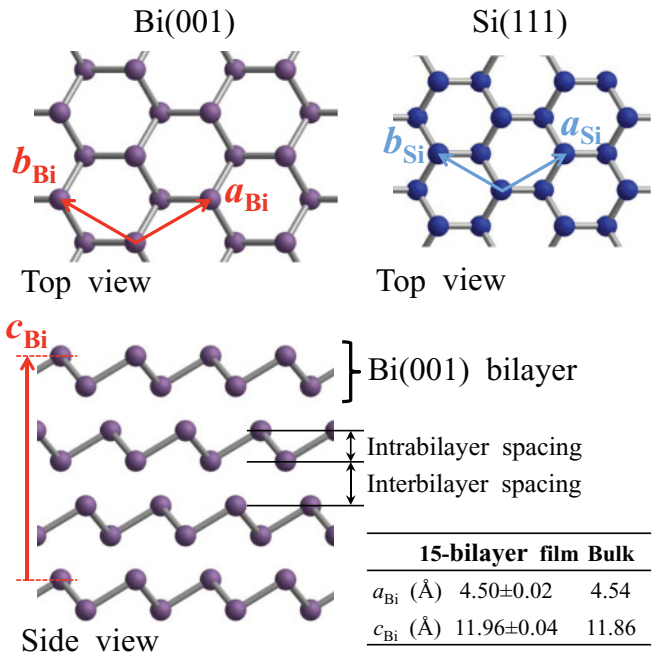

	15-bilayer film	Bulk
a_{Bi} (Å)	4.50±0.02	4.54
c_{Bi} (Å)	11.96±0.04	11.86

FIG. 1. (Color online) Ball-and-stick models of the [001]-oriented Bi and Si(111) bilayers. Basis vectors of their lattices are denoted. The bottom right table shows the lattice constants of the 15-bilayer Bi(001) film, obtained by our analysis, and their bulk values.[19]

For a definition of the Miller indices h, k, and l, the basis vectors of the real-space lattice $\boldsymbol{a}_{Bi}$, $\boldsymbol{b}_{Bi}$, and $\boldsymbol{c}_{Bi}$, denoted in the structure model of Fig. 1, are used. Throughout this paper, the bulk value of $1/c_{Bi} = 0.0843$ Å^{-1} is used as the reciprocal lattice unit (r.l.u.) of l.[19]

A Bi(001) film with a thickness of ∼15 bilayers was prepared to investigate the film structure. Nonspecular reciprocal lattice rods, (1 0), (0 1), and (1 1) rods, of the film were measured with the grazing incidence mode.[21] The x-ray glancing angle was 0.5°. For the investigation of the interface structure, another thinner film with a nominal thickness of ∼11 bilayers was prepared to increase the scattering contribution from the interface. The specular (0 0) rod of the sample was measured by using a manipulator suitable for the specular rod measurement.[22]

III. RESULTS

A. Structure of the Bi(001) film

The measured structure factors, the square root of the diffraction intensities, of the nonspecular rods of the ∼15-bilayer Bi(001) film are plotted in Fig. 2. Since the Bi(001) rods do not overlap with the Si(111) Bragg rods, the structure factors only represent the film structure, regardless of its translational relationship with the substrate. From the in-plane positions of the Bi(001) rods, the lattice constant $a_{Bi} = b_{Bi} = 4.50 \pm 0.02$ Å, compressed by 0.9% from the bulk value,[19] was obtained. This value satisfies the magic epitaxial relationship with the Si(111)-7 × 7 surface $a_{Si} \times 7/6 = 4.48$ Å within the error in agreement with the spot-profile-analyzing low-energy electron diffraction (LEED) measurement.[10]

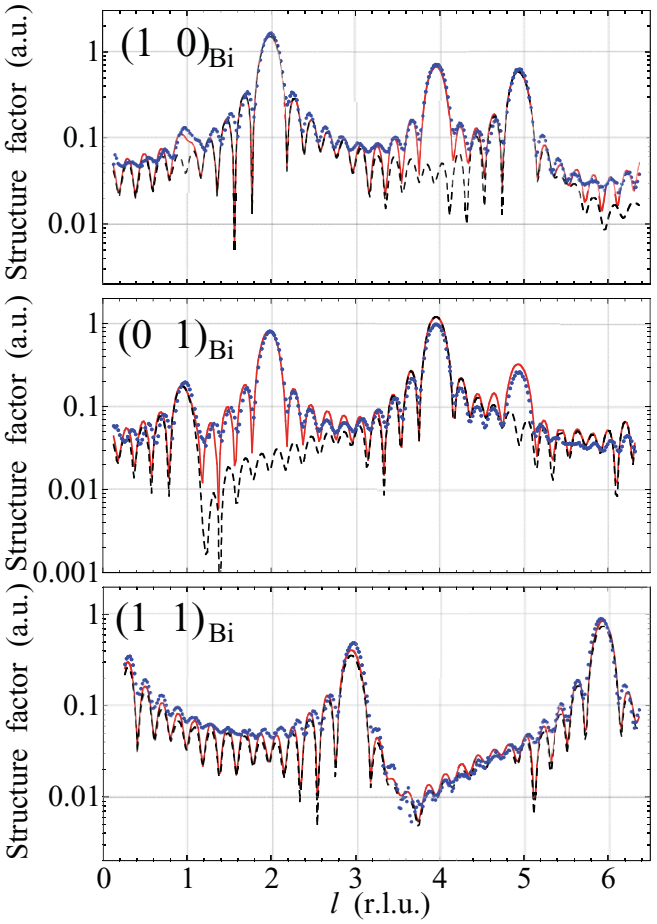

FIG. 2. (Color online) Comparison of structure factors along reciprocal lattice rods of the 15-bilayer Bi(001) film. The solid symbols are measured structure factors, the dashed curves are those calculated from a single-domain film, and the solid curves are those from the best-fit double-domain film.

The measured structure factors in Fig. 2 show Laue-function-like fringes. The (1 0) and (0 1) rods show similar oscillations, although these two rods should be inequivalent according to the $p3m1$ symmetry of the Bi(001) surface. The most probable origin of this similarity is the superposition of diffraction intensities from rotational domains, which frequently occurs in two-dimensional systems. To investigate this effect, we show structure factors calculated for a single-domain 15-bilayer Bi(001) film as dashed lines in Fig. 2. The model structure has the in-plane orientation with respect to the Si(111) surface as shown in Fig. 1. The structure factors show main Laue peaks, which satisfy the Bragg conditions of the Bi(001) film at $l \approx 2$ and $l \approx 5$ in the (1 0) rod and at $l \approx 1$ and $l \approx 4$ in the (0 1) rod. It is clear that the superposition of the calculated (1 0) and (0 1) rods can reproduce all the main Laue peaks of the experimental (1 0) or (0 1) rods. Therefore, the existence of another rotational domain, whose $\boldsymbol{a}_{Bi}$ coincides with $\boldsymbol{b}_{Bi}$ of the other domain, in the active surface area of $\sim 1 \times 8$ mm^2 is indicated. Since the {1 1} rods are symmetrically equivalent for both of the rotational domains under the $p3m1$ symmetry, the measured (1 1) rod is well reproduced by the calculation for the single-domain film. The formation of the double-domain film is apparently unreasonable

because the symmetrical restrictions that the 7×7 surface is the single-domain surface and both of the Bi(001) films and underlying 7×7 structures have the threefold rotational symmetry should make the epitaxial Bi(001) film a single domain. The reason for the double-domain formation will be discussed in Sec. IV in terms of the interface junction.

To obtain the lattice constant c_{Bi} and occupancies of the rotational domains of the 15-bilayer Bi(001) film, a least-squares structure refinement was performed. As experimental evidence for the film structure, the measured l positions of the main Laue peaks are smaller than the corresponding integer values by $\sim$1%. This directly indicates that the Bi(001) film is vertically expanded from the bulk structure by $\sim$1%. Therefore, as an initial trial structure, a 1% expanded 15-bilayer Bi(001) film, in which the Bi atoms are located at the bulk-lattice positions defined by the so-called z parameter of 0.234,[19] was used. Since obtaining full optimization of the 30 Bi atoms in the unit cell into the global minimum is a difficult task, the number of fitting parameters was reduced as much as possible. The following 20 parameters were optimized: the lattice constant c_{Bi}, an isotropic Debye-Waller factor common to all atoms, vertical relaxations for the three bilayers from the surface and the bottom, an occupancy ratio between the two rotational domains, occupancies of the topmost two bilayers for each domain, and a scale factor between the experimental values and calculated ones. Due to the magic epitaxial relationship $6 \times a_{\mathrm{Bi}} = 7 \times a_{\mathrm{Si}}$, the positions of the Bi(001) rods overlap with the Si(111)-7×7 rods. Even though weak diffraction intensities from nonoverlapping 7×7 rods could be observed from the interface, we neglected the contribution because the number of electrons in the 7×7-reconstruction layers is $\sim$1% with respect to that of the 15-bilayer Bi(001) film.

Calculated structure factors for the best-fit model are plotted with solid curves in Fig. 2. The R factor $\sum ||F_{\mathrm{exp}}| - |F_{\mathrm{calc}}|| / \sum |F_{\mathrm{exp}}|$ is 0.19. For the summation of structure factors of the two rotational domains, the absolute value sum was used because the interference sum of the structure factors did not reproduce the measured ones. This indicates that these domain sizes well exceed the coherence length of the x rays of $\sim$100 nm. The calculated curves cannot reproduce the peak-to-dip heights and the positions of subpeaks due to the simplification of the structure model well. However, the positions of the main Laue peaks, representing the average lattice constant c_{Bi} of the film, are well reproduced. The obtained c_{Bi} is 11.96 ± 0.04 Å, expanded from the bulk value by 0.8%. The occupancy ratio of the rotated domain with respect to the main one defined in Fig. 1 is 0.54 ± 0.01. The vertical relaxations at the top and bottom three bilayers are less than 5% from the bulk positions. The amplitude of atomic displacement in the isotropic Debye-Waller factor is 0.21 ± 0.03 Å, approximately three times larger than the bulk value.[19] This value includes static structural fluctuations of the film. We also tried to allow lateral relaxations of the Bi atoms, but this led to physically unreasonable positions.

B. Interface structure of Bi(001)/Si(111)-7 × 7

The interface structure was investigated by analyzing structure factors along the specular (0 0) rod, which are proportional to the Fourier transform of the electron-density distribution projected onto the z axis $\rho(z)$. Structure factors measured from the $\sim$11-bilayer Bi(001) film are plotted in Fig. 3 with two kinds of circular symbols. The data at $l < 1.47$, plotted with the light-gray symbol, were measured in such a condition that the sample surface could not fully receive the incident x-ray beam due to shallow incident angles. Although these data were corrected by the active area, they are still less reliable than those measured at higher angles ($l > 1.47$). Thus, we omitted the data at $l < 1.47$ in the following quantitative structure analyses. The sharp peaks at $l = 3.78$ and 11.35 correspond to the 111 and 333 Bragg reflections of the substrate Si.

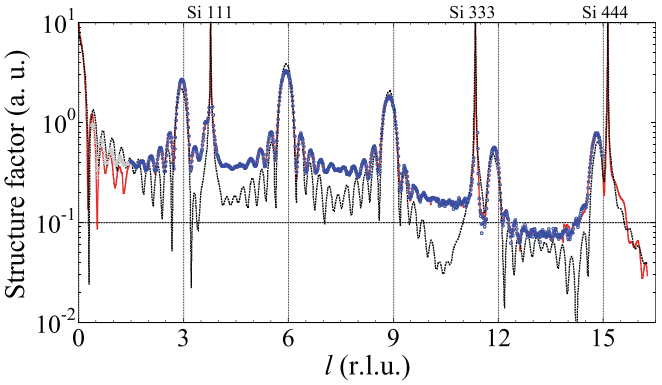

FIG. 3. (Color online) Comparison of structure factors along the specular rod of the $\sim$11-bilayer-thick Bi(001) film on the Si(111)-7×7 surface. The solid symbols are measured structure factors (the light-gray ones were not included in the analyses due to the unreliable measurement condition), the dashed curve was calculated from the least-squares-fitted model without the interfacial Bi wetting layer, and the solid curve was calculated from the coherent Bragg rod analysis-(COBRA)-derived electron densities of Fig. 5, which includes the wetting layer.

The electron-density profile $\rho(z)$ across the interface was obtained by utilizing direct methods as described in the following sections. In short, a structure model of the interface was directly constructed by using a holographic method,[23] and $\rho(z)$ of the structure model was quantitatively derived by phase-retrieval methods.[24–27]

1. *Model construction by a holographic method*

In Fig. 3, the Laue-function fringe of the (0 0) rod shows nine clear subpeaks in the range of $0 < l < 3$, indicating that at least 11 bilayers exist in the film. First, a least-squares structure refinement was performed for a simple structure model, an 11-bilayer Bi(001) film on the 7×7 surface. For the structure of the 7×7-reconstructed Si(111) bilayer, we used the electron density of the so-called dimer adatom stacking-fault (DAS) model[28] and the bulk-truncated z positions. For the height of the Si adatom from the 7×7-reconstructed layer, the average value of 1.4 Å from Table I of Ref. 29 was adopted. The 7×7 structure was fixed in the fit. The structure parameters were the interface distance between the film and the 7×7 structure, the lattice constant c_{Bi}, the occupancies of the topmost three bilayers, and the isotropic Debye-Waller factor common to all Bi atoms. The dashed curve in Fig. 3 is the calculated one for the best-fit model. The calculation well reproduces the main

Laue peaks of the Bi(001) film, indicating that, at least, the average lattice constant $c_{Bi} = 12.01$ Å is reliably obtained. This value is slightly larger than the 11.96 Å of the 15-bilayer film (see Sec. III A). This might indicate that thicker films approach the bulk value of 11.86 Å.[19] In the calculated curve of Fig. 3, deviations from the experiment are significant around the Bragg peaks of Si, where the structure factor becomes sensitive to the interference between the film and the substrate. This indicates that the simple interface junction model is incorrect.

In order to construct the interface structure model directly from the experimental data, a holographic imaging method was applied.[23] The basic idea of this method is that the scattering distribution along the reciprocal lattice rod is regarded as the interference between the reference wave F^{ref} from the known part of the sample and the object wave F^{unknown} from the unknown part. The holographic method is useful to acquire unknown additional structures at the surface[30] and the interface.[31] In the present case, the electron density $\rho(z)$ of the unknown part will be imaged in a hologram $U(z)$ given by the Fourier transform of the hologram function $\chi(l)$,

$$\chi(l) = \frac{I^{\mathrm{exp}}(l) - |F^{\mathrm{ref}}(l)|^2}{F^{\mathrm{ref}*}(l)}, \tag{1}$$

$$U(z) = \int \chi(l)\exp(-i2\pi lz)\,dl, \tag{2}$$

where $I^{\mathrm{exp}}(l)$ is the measured scattering intensity at a certain l. Here, the known parts of the structure are the substrate and the Bi(001) film, and thus, F^{ref} should become the interference sum between $F^{\mathrm{substrate}}$ and F^{film}. To calculate F^{ref}, however, the interface relationship between the substrate and the film, which is *a priori* unknown, must be known *a priori*. To avoid this contradiction, we reduced the contributions from the substrate as much as possible by simply omitting data around the Si 111 and 333 Bragg peaks in the Fourier transform of $\chi(l)$ and, thus, assumed $F^{\mathrm{ref}} = F^{\mathrm{film}}$. This assumption means that the calculated hologram reconstructs unknown parts of the reference film, hopefully an additional interface structure. The ranges of l removed in the hologram calculation are within ± 0.4 from each of the two Bragg peaks. As the reference structure, the 11-bilayer film optimized by the least-squares fit was used.

The real part of the calculated hologram Re $U(z)$ is plotted with the solid curve in Fig. 4. The $\rho(z)$ of the reference Bi(001) film obtained by the Fourier transform of F^{film} is also plotted with the dashed curve as a guide to the hologram. The hologram shows a prominent peak located at ~3.2 Å below the bottom peak of the reference film. The prominent peak always appeared at the same position regardless of the cut range of l and the modifications of the reference structure, while the other minor features were unstable. The minor features are artifacts, including conjugate images, probably caused by the uncertainties of the assumption $F^{\mathrm{ref}} = F^{\mathrm{film}}$, the reference structure, and the required condition $|F^{\mathrm{film}}(l)| \gg |F^{\mathrm{unknown}}(l)|$.[23] The stable prominent peak indicates the existence of a single atomic layer at the buried interface. The existence of the interface layer is consistent with STM observations of a rugged wetting layer at the initial stage of Bi deposition.[16,17]

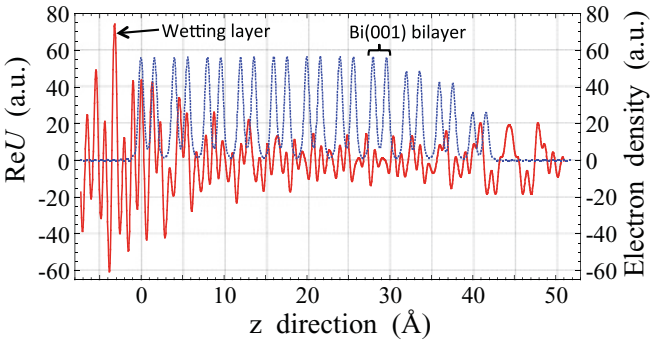

FIG. 4. (Color online) Real part of the hologram $U(z)$ calculated for the ~11-bilayer Bi(001) film (the solid curve) and electron densities of the reference film (the dashed curve). The origin of the z position is the bottom peak of the reference film. The wetting layer, reconstructed in the hologram, is indicated.

The validity of the wetting-layer model was checked by a least-squares fit. The new interface model resulted in an R factor of 0.14, which is significantly improved from 0.28 for the model without the wetting layer. The fitted interlayer distances are 2.76 ± 0.01 Å between the Si adatom and the wetting layer and 3.23 ± 0.02 Å between the wetting layer and the bottom of the film. The latter value agrees with the location of the wetting-layer peak in the hologram.

2. *Electron-density profile*

The quantitative electron-density profile $\rho(z)$ was obtained directly from the experimental data with the aid of phase-retrieval methods. We used two methods, COBRA, which utilizes a correlation between adjacent structure factors to retrieve their phases[24,25] and the *phase and amplitude recovery and diffraction image generation method* (PARADIGM), which utilizes an iterative process of alternate constraints in real and reciprocal spaces to reconstruct the electron density.[26,27] In both methods, the wetting-layer model optimized by the least-squares method was used as the initial reference structure, and the following real-space constraints were applied: The electron density $\rho(z)$ was fixed to the bulk Si(111) structure below the 7×7-reconstructed bilayer, more than 65 Å above the 7×7-reconstructed bilayer $\rho(z)$ was constrained to zero to represent the vacuum region, and negative values of $\rho(z)$ were replaced by zeros. The COBRA-derived $\rho(z)$ is shown in Fig. 5. Almost the same $\rho(z)$ was obtained by PARADIGM. The structure factors calculated from $\rho(z)$ are shown in Fig. 3 with the solid curve. The experiment is nicely reproduced with an R factor of 0.025. COBRA required two to three iterations before convergence, while PARADIGM required five to six iterations, probably due to the much stronger reciprocal space constraint in COBRA. We note that, in the present case, the resulting electron density depends on the initial reference structure. Starting from the interface model without the wetting layer, both of the methods produced unreasonable electron densities. The construction of the wetting-layer model by the holographic method and the following least-squares optimization of the wetting-layer-substrate distance were necessary steps for the phase-retrieval analyses.

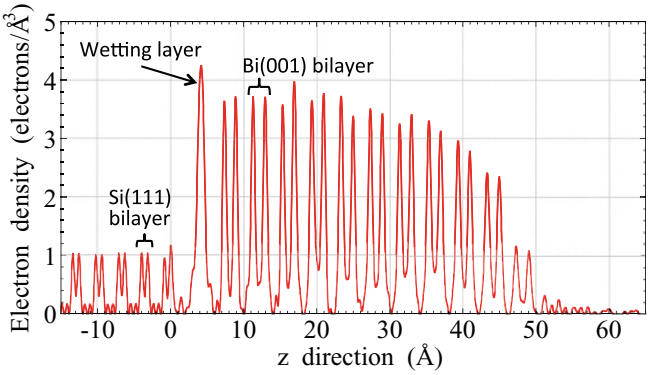

FIG. 5. (Color online) The COBRA-derived electron-density profile $\rho(z)$ of the 11-bilayer Bi(001) film on the Si(111)-7 × 7 surface. The origin of the z position is the topmost peak of the substrate.

In the resulting $\rho(z)$ of Fig. 5, the negative z region is inside the Si(111) substrate, and the positive region is the Bi(001) film. The clear paired peaks in the substrate region correspond to the Si(111) bilayers, and the larger ones in the film region correspond to the Bi(001) bilayers. Small peaks in-between the Si(111) bilayers are artificial sidelobes of the Si(111) bilayer caused by the truncation error of the finite-range Fourier transform. The most striking feature of the $\rho(z)$ is the electron-density peak between the film and the substrate, which corresponds to the wetting layer. To derive structural properties of the interface, the $\rho(z)$ was decomposed into Gaussians, assuming that the wetting layer was a single Gaussian and each of the Si(111) and Bi(001) bilayers consisted of two Gaussians. The number of electrons per Si(111)-1 × 1 mesh (Gaussian area), the interlayer spacing, the width of the atomic layers (full width at half maximum (FWHM) of Gaussian), derived by the Gaussian decomposition are plotted in Fig. 6. The layer number zero corresponds to the wetting layer, and the positive layer numbers correspond to the atomic layers within the film. Here, the Si adatom layer of the 7 × 7 structure is not counted because its small electron density, ∼6% with respect to a Bi(001) atomic layer, can be significantly affected by the sidelobes of the wetting layer and the topmost layer of the substrate. We only mention that, in Fig. 5, a small isolated peak is located at 1.4 Å above the substrate as the Si adatom in the reference structure.

Before proceeding to the discussion of the electron density $\rho(z)$, we inspect the quality of the analysis. Taking account of the anomalous scattering corrections to the x-ray atomic scattering factor for the 11-keV x rays, the number of electrons per atom becomes 76.6 for Bi and 14.16 for Si. Therefore, the expected number of electrons per Si(111)-1 × 1 mesh in a Bi(001) atomic layer is 56.2, considering the 6/7 magic epitaxial relationship. This value is indicated by the dashed line in Fig. 6(a). From the 1st to the 16th layer, the number of electrons agrees with the expected value with a standard deviation of 4.9 electrons. The gradual decay in the number of electrons toward the surface represents the thickness distribution of the sample as seen elsewhere.[25,32] The dashed lines in Fig. 6(b) represent the intrabilayer spacing of 1.61 Å and the interbilayer spacing of 2.38 Å of bulk Bi(001) with the lattice constant $c_{Bi} = 12.01$ Å. The definitions of the spacings

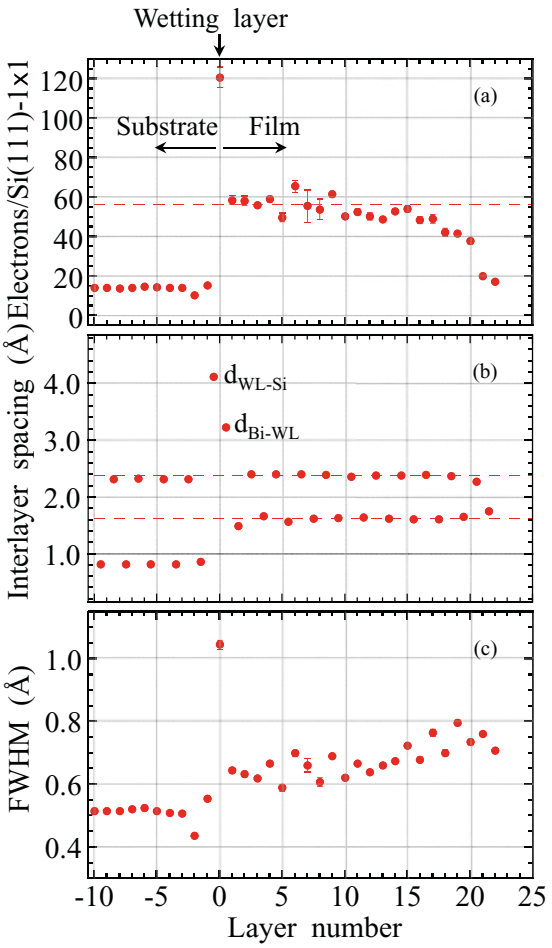

FIG. 6. (Color online) (a) The number of electrons in each atomic layer, (b) interlayer spacing, and (c) width of each atomic layer of the 11-bilayer Bi(001) film on the Si(111)-7 × 7 surface, obtained from the electron-density profile of Fig. 5. The positive (negative) layer numbers correspond to atomic layers in the film (substrate). The position of the wetting layer is indicated at the top. The dashed line in (a) represents the expected number of electrons in a Bi(001) atomic layer. The dashed lines in (b) represent the interbilayer spacing 2.38 Å and the intrabilayer spacing 1.61 Å of the bulk structure with $c_{Bi} = 12.01$ Å.

are given in Fig. 1. The interlayer spacings of the $\rho(z)$ agree with the bulk values with a standard deviation of 0.03 Å for the intrabilayer spacing and 0.02 Å for the interbilayer spacing, except for the surface and interface bilayers. These reasonable structural properties of the $\rho(z)$ support the validity of the analysis. Concerning the widths of the electron-density peaks shown in Fig. 6(c), we note that these are not the true atomic-layer widths but those convoluted with a real-space broadening function determined by the range of the x-ray diffraction data. In the present paper, the broadening is ∼0.4 Å, given by the range of the (0 0) rod data extending to about $l = 5$. In the case of the wetting layer, however, since its width of 1.04 Å is larger than twice the broadening, it is not affected by the broadening function. Actually, we confirmed, by test calculations with different broadening functions (different reciprocal space ranges in the Fourier transform), that the wetting layer width is the true one. The test calculations also

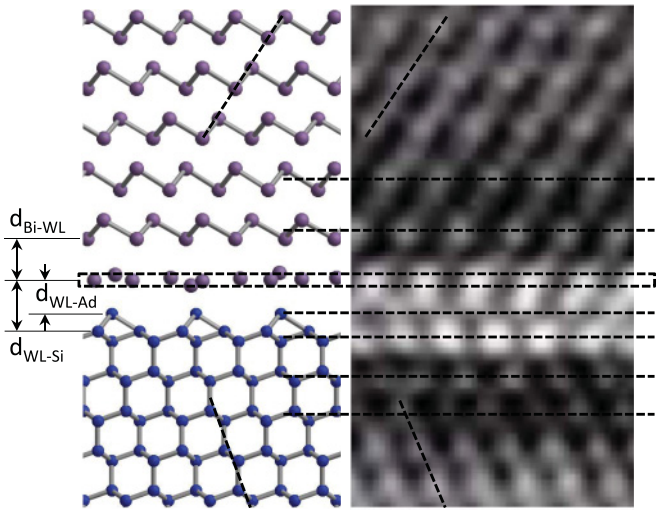

FIG. 7. (Color online) Structure model of the Bi(001)/Si(111)-7 × 7 interface, constructed from the structure analysis. The interlayer spacings $d_{\text{Bi-WL}}$, $d_{\text{WL-Ad}}$, and $d_{\text{WL-Si}}$ are defined. The right panel shows a part of the TEM image of Ref. 18 for comparison with the structure model.

showed that the Si(111) layers were widened on the order of 0.1 Å and the Bi(001) layers on the order of 0.01 Å.

IV. DISCUSSION

We constructed the interface structure model as in Fig. 7 on the basis of the structure analysis. The number of electrons in the wetting layer is 120 ± 5, corresponding to 2.13 ± 0.09 Bi atoms per Bi(001)-1 × 1 mesh. This value is not largely different from that in the initial stage wetting layer, ∼1.6 (equivalent to ∼1 monolayer of the Bi{012} layer), estimated by the STM studies.[16,17] Assuming that all the Bi atoms are packed in the same height with the close-packed form, the in-plane Bi-Bi distance becomes 3.1 ± 0.1 Å, close to the bond length of 3.06 Å in the bulk. In the interface model of Fig. 7, the wetting-layer atoms are vertically corrugated within ±0.52 Å, based on the obtained atomic-layer width of 1.04 Å. The Si adatom layer is placed at 1.4 Å above the substrate. Note that, because the present analysis could not derive the relative lateral positions among the wetting layer, film, and substrate, these positions are arbitrary in the model. The lateral positions of the wetting-layer atoms are intentionally arranged to represent their agglomerating features.[16,17] The right panel of Fig. 7 shows the TEM image of Ref. 18. Assuming that the brighter layers of the TEM image consist of the 7 × 7-reconstructed layer, Si adatom layer, and the wetting layer, their vertical positions are nicely reproduced by our structure model.

The relevant interlayer spacings $d_{\text{Bi-WL}}$, $d_{\text{WL-Ad}}$, and $d_{\text{WL-Si}}$ are defined in Fig. 7. The spacing between the bottom of the Bi(001) film and the wetting layer $d_{\text{Bi-WL}}$ is 3.23 Å, larger than the bulk interbilayer spacing by 0.85 Å. The Bi(001) structure is a layered structure, covalentlike intrabilayer bonds, and van der Waals-like interbilayer bonds. Therefore, the large $d_{\text{Bi-WL}}$ indicates a very weak interaction between the Bi(001) film and the wetting layer. The top and bottom layers showed no sign of reconstruction structure, instead, they exhibited vertical relaxations as seen in Fig. 6(c). The intrabilayer spacings are contracted by 8% at the bottom bilayer and 8% expanded at the surface, and the interbilayer spacing is contracted by 5% at the surface. Neglecting the small vertical relaxations, the film can be regarded as an inversion-symmetric structure along the z direction. Hirahara *et al.* observed spin-degenerate quantum well states, which were expected to exhibit Rashba-type spin splitting if the vacuum-film and film-substrate interfaces had inequivalent structures.[12,13] The spin-degenerate electronic states are well reproduced by *ab initio* calculations for free-standing Bi(001) slabs.[12,13] The present result directly shows that the Bi(001) film is in the nearly inversion-symmetric free-standing state.

The strength of the interaction between the wetting layer and the substrate is indicated by the interlayer spacings $d_{\text{WL-Si}}$ and $d_{\text{WL-Ad}}$. The spacing between the wetting layer and the substrate $d_{\text{WL-Si}}$ is 4.12 Å, close to the summation of the van der Waals radii of Si and Bi, 4.17 Å,[33] indicating a weak interaction between them. On the other hand, the spacing between the wetting layer and the Si adatom layer $d_{\text{WL-Ad}}$ is ∼2.7 Å, close to the summation of the covalent radii of Si and Bi, 2.59 Å,[34] indicating their much stronger interactions. These wetting-layer-substrate interactions are consistent with the STM observations on the initial stage of Bi deposition in which Bi atoms agglomerate preferably around the Si adatoms without affecting the 7 × 7-reconstructed layer.[16,17] The STM studies also showed that there is no nucleation preference and shape difference for the Bi agglomerates between the faulted and the unfaulted halves of the 7 × 7 structure. These facts indicate that the wetting layer inherits the 7 × 7-periodic potential but buffers the potential difference between the half-units of the 7 × 7. Therefore, the Bi(001) film feels the 7 × 7-periodic potential with a nearly sixfold rotational symmetry from the wetting layer, through their weak interaction. This picture simply explains why the Bi(001) film, with a threefold symmetry, can grow on the single-domain 7 × 7 surface with the two opposite in-plane orientations. The biased ratio of the domain population 0.54, obtained for the 15-bilayer Bi(001) film (see Sec. III A), indicates that a weak threefold symmetry actually persists in the wetting layer and that the film prefers the orientational relationship shown in Fig. 1.

The preference in the film orientation was observed for all samples. However, we never succeeded in preparing the complete single-domain Bi(001) film even in a vacuum chamber in our laboratory where the vacuum pressure was $\sim 10^{-8}$ Pa during the Bi deposition. The laboratory-based samples exhibited clear threefold symmetry LEED patterns. However, intensity versus energy spectra of the symmetrically inequivalent spots showed similar curves with different intensities, in the same way as the XRD measurements [cf. (1 0) and (0 1) rods in Fig. 2]. Therefore, both of the rotational domains exist within the electron-beam size of ∼1 mm ϕ. It is probably difficult to grow a single-crystal domain, which extends more than ∼1 mm^2. Therefore, we strongly recommend an examination of single crystallinity of the film prior to detailed discussions on symmetry-related properties. For example, in Refs. 7 and 9, the magnitude of the spin polarization of the surface states might have been reduced by the existence of rotated domains if the probe area exceeded the domain size, although this effect does not

upset their main conclusions. The quality of these samples had been checked by observations of electron-diffraction patterns without measuring the rod intensity profiles. We note that apparent threefold symmetry diffraction patterns do not necessarily prove the single crystallinity.

V. CONCLUSIONS

The Bi(001)/Si(111)-7 × 7 structure was revealed by the surface XRD. The determined lattice constants of the 15-bilayer Bi(001) film at room temperature satisfy the magic epitaxial relationship $6|\boldsymbol{a}_{\mathrm{Bi}}| = 7|\boldsymbol{a}_{\mathrm{Si}}|$ and show that the film is vertically expanded by ∼0.8% from the bulk structure.[19] The interface structure was determined by the direct methods in structure analysis. The interfacial wetting layer was clearly reconstructed, and the TEM image of the interface[18] can be well interpreted. The obtained interface spacings in the wetting layer, the film, and the substrate show that the film is nearly free standing without breaking the space-inversion symmetry. The coexistence of two rotational domains was observed in all the samples, suggesting that a careful evaluation of the single crystallinity is necessary prior to quantitative studies on symmetry-related phenomena.

ACKNOWLEDGMENTS

This work was supported by a Grant-in-Aid for Scientific Research (Grant No. 22360018) from JSPS. The synchrotron radiation experiments were performed at beamline 15B2 of the Photon Factory, KEK, under the approval of the Photon Factory Program Advisory Committee Proposals No. 2009G612 and No. 2010G079. T.S. thanks Y. Wakabayashi for helpful advice and discussions on the COBRA analysis.

*sirasawa@issp.u-tokyo.ac.jp

[1] G. E. Smith, G. A. Baraff, and J. M. Rowell, Phys. Rev. A **135**, 1118 (1964).
[2] V. B. Sandomirskii, Sov. Phys. JETP **25**, 101 (1967).
[3] F. Y. Yang, K. Liu, K. Hong, D. H. Reich, P. C. Searson, and C. L. Chien, Science **284**, 1335 (1999).
[4] Y. M. Koroteev, G. Bihlmayer, J. E. Gayone, E. V. Chulkov, S. Blügel, P. M. Echenique, and P. Hofmann, Phys. Rev. Lett. **93**, 046403 (2004).
[5] J. I. Pascual, G. Bihlmayer, Y. M. Koroteev, H.-P. Rust, G. Ceballos, M. Hansmann, K. Horn, E. V. Chulkov, S. Blügel, P. M. Echenique, and P. Hofmann, Phys. Rev. Lett. **93**, 196802 (2004).
[6] P. Hofmann, Prog. Surf. Sci. **81**, 191 (2006).
[7] T. Hirahara, K. Miyamoto, I. Matsuda, T. Kadono, A. Kimura, T. Nagao, G. Bihlmayer, E. V. Chulkov, S. Qiao, K. Shimada, H. Namatame, M. Taniguchi, and S. Hasegawa, Phys. Rev. B **76**, 153305 (2007).
[8] A. Kimura, E. E. Krasovskii, R. Nishimura, K. Miyamoto, T. Kadono, K. Kanomaru, E. V. Chulkov, G. Bihlmayer, K. Shimada, H. Namatame, and M. Taniguchi, Phys. Rev. Lett. **105**, 076804 (2010).
[9] A. Takayama, T. Sato, S. Souma, and T. Takahashi, Phys. Rev. Lett. **106**, 166401 (2011).
[10] T. Nagao, J. T. Sadowski, M. Saito, S. Yaginuma, Y. Fujikawa, T. Kogure, T. Ohno, Y. Hasegawa, S. Hasegawa, and T. Sakurai, Phys. Rev. Lett. **93**, 105501 (2004).
[11] T. Hirahara, T. Nagao, I. Matsuda, G. Bihlmayer, E. V. Chulkov, Yu. M. Koroteev, P. M. Echenique, M. Saito, and S. Hasegawa, Phys. Rev. Lett. **97**, 146803 (2006).
[12] T. Hirahara, T. Nagao, I. Matsuda, G. Bihlmayer, E. V. Chulkov, Yu. M. Koroteev, and S. Hasegawa, Phys. Rev. B **75**, 035422 (2007).
[13] T. Hirahara, K. Miyamoto, A. Kimura, Y. Niinuma, G. Bihlmayer, E. V. Chulkov, T. Nagao, I. Matsuda, S. Qiao, K. Shimada, H. Namatame, M. Taniguchi, and S. Hasegawa, New J. Phys. **10**, 083038 (2008).
[14] T. Hirahara, Y. Sakamoto, Y. Saisyu, H. Miyazaki, S. Kimura, T. Okuda, I. Matsuda, S. Murakami, and S. Hasegawa, Phys. Rev. B **81**, 165422 (2010).
[15] J. T. Sadowski, T. Nagao, S. Yaginuma, Y. Fujikawa, A. Al Mahboob, K. Nakajima, and T. Sakurai, Appl. Phys. Lett. **86**, 083109 (2005).
[16] J. T. Sadowski, T. Nagao, S. Yaginuma, Y. Fujikawa, T. Sakurai, A. Oreshkin, M. Saito, and T. Ohno, J. Appl. Phys. **99**, 014904 (2006).
[17] T. Nagao, T. Doi, T. Sekiguchi, and S. Hasegawa, Jpn. J. Appl. Phys., Part 1 **39**, 4567 (2000).
[18] T. Nagao, S. Yaginuma, M. Saito, T. Kogure, J. T. Sadowski, T. Ohno, S. Hasegawa, and T. Sakurai, Surf. Sci. **590**, L247 (2005).
[19] P. Cucka and C. S. Barrett, Acta. Cryst. **15**, 865 (1962).
[20] E. Vlieg, J. Appl. Crystallogr. **30**, 532 (1997).
[21] M. Takahasi, S. Nakatani, Y. Ito, T. Takahashi, X.-W. Zhang, and M. Ando, Surf. Sci. **357-358**, 78 (1996).
[22] K. Sumitani, K. Masuzawa, T. Hoshino, S. Nakatani, T. Takahashi, H. Tajiri, K. Akimoto, H. Sugiyama, X.-W. Zhang, and H. Kawata, Appl. Surf. Sci. **252**, 5288 (2006).
[23] T. Takahashi, K. Sumitani, and S. Kusano, Surf. Sci. **493**, 36 (2001).
[24] Y. Yacoby, M. Sowwan, E. Stern, J. O. Cross, D. Brewe, R. Pindak, J. Pitney, E. M. Dufresne, and R. Clarke, Nature Mater. **1**, 99 (2002).
[25] M. Sowwan, Y. Yacoby, J. Pitney, R. MacHarrie, M. Hong, J. Cross, D. A. Walko, R. Clarke, R. Pindak, and E. A. Stern, Phys. Rev. B **66**, 205311 (2002).
[26] D. K. Saldin, R. J. Harder, V. L. Shneerson, and W. Moritz, J. Phys.: Condens. Matter **13**, 10689 (2001).
[27] D. K. Saldin and V. L. Shneerson, J. Phys.: Condens. Matter **20**, 304208 (2008).
[28] K. Takayanagi, Y. Tanishiro, S. Takahashi, and M. Takahashi, Surf. Sci. **164**, 367 (1985).
[29] A. Kawasuso, Y. Fukaya, K. Hayashi, M. Maekawa, S. Okada, and A. Ichimiya, Phys. Rev. B **68**, 241313(R) (2003).
[30] K. Sumitani, T. Takahashi, S. Nakatani, A. Nojima, O. Sakata, Y. Yoda, S. Koh, T. Irisawa, and Y. Shiraki, Jpn. J. Appl. Phys., Part 2 **42**, L189 (2003).

[31] T. Takahashi, T. Shirasawa, K. Sekiguchi, and W. Voegeli, e-J. Surf. Sci. Nanotechnol. **7**, 525 (2009).

[32] D. D. Fong, C. Cionca, Y. Yacoby, G. B. Stephenson, J. A. Eastman, P. H. Fuoss, S. K. Streiffer, C. Thompson, R. Clarke, R. Pindak, and E. A. Stern, Phys. Rev. B **71**, 144112 (2005).

[33] M. Mantina, A. C. Chamberlin, R. Valero, C. J. Cramer, and D. G. Truhlar, J. Phys. Chem. A **113**, 5806 (2009).

[34] B. Cordero, V. Gómez, A. E. Platero-Prats, M. Revés, J. Echeverría, E. Cremades, F. Barragán, and S. Alvarez, Dalton Trans. 2832 (2008).